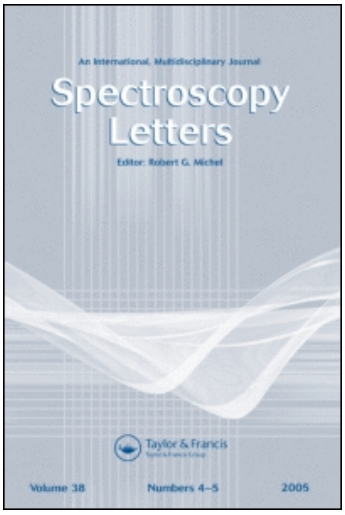

Spectroscopy Letters
Publication details, including instructions for authors and subscription information:
http://www.informaworld.com/smpp/title~content=t713597299

The Efficiency of Corrosion Inhibitor as Given by Electrochemical Impedance Spectroscopy Tafel Polarization and Weight-Loss Measurements

I. Forsal[a]; L. Lakhrissi[b]; K. Naji[b]; S. Abirou[c]; M. Ebn Touhami[a]; B. Lakhrissi[b]; M. Addou[c]
[a] Laboratoire d'électrochimie, de corrosion et d'environnement, Université Ibn Tofail, Faculté des Sciences, Kénitra, Morocco [b] Laboratoire d'Agroressources et Génie des Procédés, Université Ibn Tofail, Faculté des Sciences, Kénitra, Morocco [c] Laboratoire d'Optoélectronique et de Physico-chimie des Matériaux, Université Ibn Tofail, Faculté des Sciences, Kénitra, Morocco

Online publication date: 17 March 2010

To cite this Article Forsal, I. , Lakhrissi, L. , Naji, K. , Abirou, S. , Touhami, M. Ebn , Lakhrissi, B. and Addou, M.(2010) 'The Efficiency of Corrosion Inhibitor as Given by Electrochemical Impedance Spectroscopy Tafel Polarization and Weight-Loss Measurements', Spectroscopy Letters, 43: 2, 136 — 143
To link to this Article: DOI: 10.1080/00387010903261180
URL: http://dx.doi.org/10.1080/00387010903261180

Spectroscopy Letters, 43:136–143, 2010

ISSN: 0038-7010 print/1532-2289 online
DOI: 10.1080/00387010903261180

Taylor & Francis
Taylor & Francis Group

The Efficiency of Corrosion Inhibitor as Given by Electrochemical Impedance Spectroscopy Tafel Polarization and Weight-Loss Measurements

I. Forsal[1], L. Lakhrissi[2], K. Naji[2], S. Abirou[3], M. Ebn Touhami[1], B. Lakhrissi[2], and M. Addou[3]

[1]Laboratoire d'électrochimie, de corrosion et d'environnement, Université Ibn Tofail, Faculté des Sciences, Kénitra, Morocco
[2]Laboratoire d'Agroressources et Génie des Procédés, Université Ibn Tofail, Faculté des Sciences, Kénitra, Morocco
[3]Laboratoire d'Optoélectronique et de Physico-chimie des Matériaux, Université Ibn Tofail, Faculté des Sciences, Kénitra, Morocco

ABSTRACT The compound 6-methylquinoxalin-2(1*H*)-one (Q-CH_3) was synthesized, and its inhibiting action on the corrosion of mild steel in 1M HCl was investigated by various corrosion-monitoring techniques: electrochemical and weight-loss measurements. Results showed that this compound has fairly good inhibiting properties for steel corrosion in acidic medium, with efficiencies of around 97% at a concentration of 10^{-2} M. The protection efficiency of this inhibitor decreases slightly with the rise of temperature, and it is improved with the immersion time.

KEYWORDS adsorption, corrosion inhibition, electrochemical impedance spectroscopy, 6-methylquinoxalin-2(1*H*)-one, 1M HCl, mild steel, thermodynamic parameters

INTRODUCTION

Steel is a widely used material in various industrial sectors because of its economic and technical properties, though its resistance to corrosive attacks from its environment remains weak. Several researchers have focused their attention on the use of the most effective inhibitors that don't have harmful effects,[1–6] especially to protect steel in an acidic medium.

Generally, the diminution of the corrosion rate is a result of adsorption, which in acidic media effectively blocks the actives sites of metal dissolution and/or hydrogen evolution. The adsorption requires the existence of attractive forces between the adsorbate and the metal. The principal types of interaction between an organic inhibitor and metal surface are physisorption, chemisorption, or both of them. The adsorption of inhibitor is influenced by the nature and surface charge of the metal, the type of aggressive electrolyte, temperature, and the chemical structure of the inhibitor. Indeed, specific interaction between functional groups and the metal surface and heteroatom like nitrogen, oxygen, sulfur, and phosphorus plays an important role in inhibition due to the free electron pairs they posses.[7] Compounds that contain π bonds generally exhibit good inhibitive properties by supplying electrons via

Received 13 November 2008; accepted 17 June 2009.

Address correspondence to I. Forsal, Laboratoire d'électrochimie, de corrosion et d'environnement, Université Ibn Tofail, Faculté des Sciences, Kénitra, Morocco. E-mail: forsalissam@yahoo.fr

the π orbital. When both of these features combine, enhanced inhibition can be observed.

The present study was undertaken to investigate the mild steel corrosion inhibition in molar hydrochloric acid by 6-methylquinoxalin-2(1*H*)-one (denoted hereafter as *Q-CH$_3$*). The study was conducted by weight loss, polarization, and impedance methods. The thermodynamic parameters of Q-CH$_3$ molecule adsorption onto mild steel were determined, and the nature of inhibitor adsorption process was also studied and discussed.

EXPERIMENTAL PROCEDURE

Synthesis of the Q-CH$_3$ Compound

Q-CH$_3$ has already been synthesized as reported elsewhere[8] with a mixed solution of 3-methyl-*o-phenylenediamine* **1** (4.32 g, 40 mmol) and *glyoxylic acid* **2** (4.6 g, 50 mmol) in *n*-butanol (120 mL) refluxed for 5 hr. After standing in a freezer for one night, the solid formed was filtered under reduced pressure and washed with *n*-hexane (20 mL) to give crystal of 6-methyl-2(1*H*)-quinoxalinone **3** (3.24 g, yield 51%; mp 196–197°C).

The product was recrystallized in a mixed solvent of dimethylformamide (DMF) and ethanol (vol. 3 : 7). The ^{1}H NMR and IR spectral data of the product are as follows:

IR (KBr) ν cm^{-1}: (NH, s), 3445 (C=O, s), 1633.

^{1}H NMR (300 MHz, DMSO) δ ppm: (s, H-3, NH), 8.18–12.40 (m, H-arom), 7.30–7.80 2.29 (d, CH_3).

The reaction mechanism is as follows:

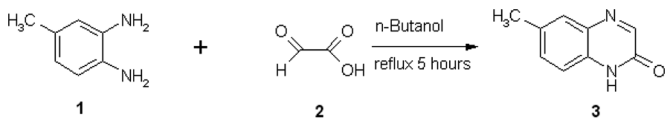

1 2 3

3 : QCH$_3$

Gravimetric, Steady-State, and EIS Measurements

Prior to all measurements, the mild steel samples (0.03% P, 0.4% Mn, 0.08% C, 0.03% S, and balance iron) were mechanically polished on wet SiC paper successively from 400 to 1200 grade. The specimens were washed thoroughly with bidistilled water, decreased ultrasonically in ethanol, and finally dried with acetone at room temperature before being immersed in the acid solution. The aggressive medium (1M HCl) was prepared by dilution of analytical grade 37% HCl.

Gravimetric experiments were carried out in double-walled glass cell. The solution volume was 100 mL. The mild steel specimens used had rectangular form (1 cm × 4 cm × 0.06 cm). The immersion time for the weight loss was 24 hr at 293 ± 1 K. The rinse removed loose segments of corroded sample's film. Triplicate experiments were performed in each case, and the mean value of the weight loss is reported. Weight loss allowed us to calculate the mean corrosion rate as expressed in mg cm^{-2} hr^{-1}.

Electrochemical measurements were investigated in a conventional three-electrode electrolysis cylindrical Pyrex glass cell equipped with thermostat-cooling condenser. The working electrode (WE), in the form of a disc cut from steel, had a geometrical area of 1 cm^2 and was embedded in polytetrafluoroethylene (PTFE) to avoid any infiltration of electrolyte. A satured calomel electrode (SCE) and a platinum electrode were used as reference electrode and auxiliary electrode, respectively. The temperature was thermostatically controlled at 293 K.

The polarization curves were recorded with a digital potentiostat type Voltalab PGZ 100 and controlled with analysis software (Voltamaster 4), at a scan rate of 1 mV s^{-1}. The mild steel electrode was maintained at open circuit conditions (corrosion potential, E_{corr}) for 30 min and thereafter prepolarized at −800 mV for 10 min. After this scan, the potential was swept to anodic potentials.

The electrochemical impedance spectroscopy (EIS) measurements were performed using a transfer function analyzer (Voltalab PGZ 100), with a small amplitude AC signal (10 mV rms) over a frequency domain from 100 kHz to 10 mHz at 293 K with 10 points per decade. Computer programs automatically controlled the measurements performed at rest potentials after 30 min of immersion at E_{corr}. The impedance diagrams were given in the Nyquist representation. In order to ensure reproducibility, all experiments were repeated three times. The evaluated inaccuracy did not exceed 10%.

RESULTS AND DISCUSSION

Weight-Loss Tests

Gravimetric measurements of mild steel were investigated in 1M HCl in the presence and absence

of various concentrations of Q-CH_3 at 24 hr of immersion and 293 K. The mass loss is determined after removing the corrosion products from the metal solution in accordance with the procedure recommended by ASTM G1-67. The values of the corrosion rate (W) and inhibiting efficiency (E_W(%)) are given in Table 1. E_W(%) was estimated by the following relation:[1]

$$E_W(\%) = \frac{W_{corr} - W_{corr/inh}}{W_{corr}} \times 100 \qquad (1)$$

Where W_{corr} and $W_{corr/inh}$ are the corrosion rates of steel without and with inhibitor, respectively. The corrosion rate of mild steel was calculated by the relation[2]

$$W = \frac{\Delta m}{St} \qquad (2)$$

Where Δm, S, and t represented the weight loss, the exposed area of specimen, and experimental time, respectively.

It is clear that the steel corrosion rate values decrease with the concentration of Q-CH_3 and that in turn the inhibiting efficiency increases to reach 97% at 10^{-2} mol L^{-1}. Its efficiency is already as high as 82% when only 10^{-3} mol L^{-1} was present in the solution.

Current–Voltage Characteristics

Curves obtained in the presence and absence of Q-CH_3 inhibitor, after prepolarizing the electrode at its E_{corr} for 30 min, are shown in Fig. 1. The potential was swept stepwise from the most cathodic potential to the anodic direction. This avoided electrolyte pollution by undergoing oxidation of iron. The current-potential plots recorded in the vicinity of E_{corr} give the corresponding polarization resistance, R_P, of mild steel in 1M HCl in the presence of various concentrations of Q-CH_3. Table 2 exemplifies the values of the associated electrochemical parameters (corrosion potentials, E_{corr}, cathodic Tafel slopes (β_c), corrosion current density (i_{corr}), polarization resistances (R_P), and inhibiting efficiencies (E_I (%) and E_{R_P}(%)). The following relations (3 and 4) determine E_I (%) and E_{R_P}%, respectively:

$$E_I\ \% = \frac{i_{corr} - i_{corr/inh}}{i_{corr}} \times 100, \qquad (3)$$

$$E_{R_P}\ \% = \frac{R_P - R'_P}{R_P} \times 100, \qquad (4)$$

where i_{corr} and $i_{corr/inh}$ are the corrosion current densities values without and with Q-CH_3, respectively determined by extrapolation of cathodic Tafel lines to the corrosion potential. R_P and R'_P are the polarization resistances with and without Q-CH_3, respectively.

It is clear that the current density decreases with increasing of the concentration; this indicates that this compound is adsorbed on the metal surface and hence inhibition occurs. Figure 1 indicates that the cathodic current-potential curves give rise to Tafel lines, indicating that the hydrogen evolution reaction is activation controlled. In contrast, the anodic curves show that the inhibition mode of organic compound depends upon electrode potential. Indeed, for an overvoltage higher than −250 mV_{sce}, the presence of Q-CH_3 does not change the current-potential characteristics, meaning that the significant steel dissolution dominates the adsorption of the inhibiting film. Therefore, in the vicinity of

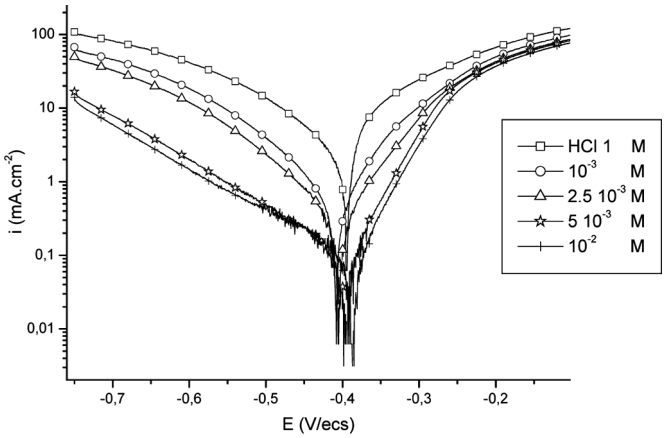

FIGURE 1 **Polarization curves for mild steel in 1M HCl containing different concentrations of Q-CH_3 at 298 K.**

TABLE 1 **Gravimetric Results of the Mild Steel Corrosion Without and With Addition of Q-CH_3 Molecules Studied at 293 K After 24 h of Immersion in 1M HCl**

Inhibitor	Concentration (mol L^{-1})	W (mg cm^{-2} h^{-1})	E_W (%)
Blank	0	8.569	—
Q-CH_3	10^{-3}	1.612	82
	2.5×10^{-3}	1.337	90
	5×10^{-3}	0.485	95
	10^{-2}	0.211	97

TABLE 2 **Values of Electrochemical Parameters Evaluated From the Cathodic Current-Voltage Characteristics for the System Electrode for 1M HCl With Added Inhibitor at 293 K**

Inhibitor	Concentration (mol L^{-1})	E_{corr}(mV_{sce})	$\lvert\beta_c\rvert$ (mV dec^{-1})	i_{corr} ($\mu A\,cm^{-2}$)	R_P ($\Omega\,cm^2$)	E_I(%)	E_{R_P}(%)	θ
Blank	0	−396	125	1072	10	—	—	—
Q-CH3	10^{-3}	−410	112	508	31	53	67	0.53
	2.5×10^{-3}	−406	106	312	52	71	80	0.71
	5×10^{-3}	−397	129	76	280	93	96	0.93
	10^{-2}	−388	136	74	291	93	97	0.93

E_{corr} and below $-250\,mV_{sce}$, the increase of Q-CH_3 concentration leads to a decrease in the current density. In this case, the adsorption rate of Q-CH_3 remains higher than its desorption rate. For anodic polarization in the presence of 1M HCl (Fig. 2), a voltage higher than −250 mV shows little effect on the presence of inhibitor when the potential became more positive than the desorption potential (Ed), −250 mV (Fig. 2). B. El Mehdi et al.[9], explained that the inhibition mode of the inhibitor was dependent on the electrode potential. This is probably due to the increase in surface area as steel dissolves and organic compound desorbes. The behavior of the inhibitor at potentials higher than −250 mV may be the result of significant dissolution of the steel surface, leading to desorption of the adsorbed inhibitor from the electrode surface. In this case, the desorption rate of the inhibitor is higher than its adsorption rate. However, the inhibitor influences the anodic reaction at potentials more negative than −250 mV. Both the anodic and cathodic current densities were decreased, and thus Q-CH_3 suppressed both the anodic and cathodic reactions, although mainly the cathodic one. It can also be seen from the experimental results that Q-CH_3 decreased i_{corr}, and in contrast it enhanced R_P significantly at all the study's concentrations. E_{R_P}% and E_I (%) are in very good agreement and indicate the excellent effect of Q-CH_3 as corrosion inhibitor on the mild steel in 1M HCl medium. It is to be noted that the Tafel slope in uninhibited medium is very comparable to that obtained in the literature.[10] The unchanged Tafel slopes (β_c) in the presence of Q-CH_3 indicating the inhibitor acted by merely blocking the reaction sites of the metal surface without changing the cathodic reaction mechanism of hydrogen discharge.

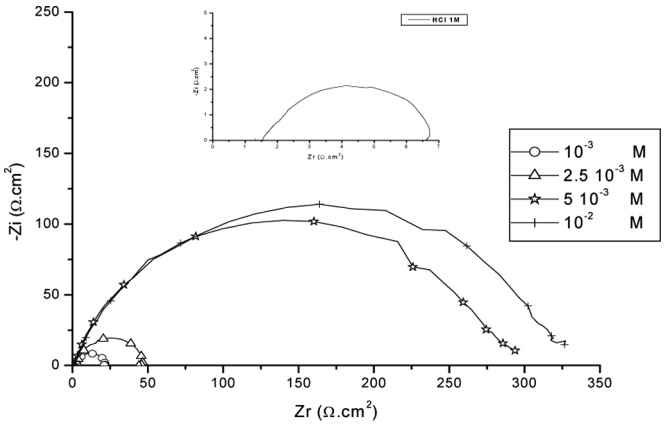

FIGURE 2 **Impedance diagrams under open circuit conditions for an immersion time of 30 min: Mild steel in 1-M HCl containing different concentrations of inhibitor Q-CH_3.**

Results of EIS Measurements

A better understanding of the mechanisms taking place at the electrode surface was attained though EIS measurements. The EIS impedance was performed under potentiostatic conditions at E_{corr} in the uninhibited and inhibited acidic solution containing various concentrations of Q-CH_3. Before each measurement, the electrode was left at the open circuit conditions during 30 min. The electrode system did not evolve significantly during the impedance measurements. The impedance diagrams obtained are characterized by a capacitive behavior (Fig. 2).

A depressed semicircle, as often obtained in acidic media[11–13] can be seen. The difference from theoretical results is generally attributed to Cole-Cole[14,15] and/or Cole-Davidson[16] representations inherent to frequency dispersion, generally attributed to the generation of micro roughness at the surface during the corrosion process.[17,18] The existence of a single semicircle relates the presence of single charge-transfer process, which is unaffected by the presence of Q-CH_3. According to a classical method, the EIS spectra of Fig. 2 will be interpreted in terms of parallel $R_t - C_d$ circuit; i.e., one time constant τ_t. Table 3 summarize the impedance parameters and values of E_{R_t}%.

TABLE 3 EIS Data of Mild Steel in 1M HCl Containing Different Concentrations of Q-CH_3 at 293 K

Concentration (mol L^{-1})	R_t ($\Omega\,cm^2$)	C_d ($\mu F\,cm^{-2}$)	E_{R_t} (%)
Blank	6	561	—
10^{-3}	25	119	76
2.5×10^{-4}	48	75	87
5×10^{-3}	297	30	98
10^{-2}	329	27	98

The results described below can be interpreted in terms of the equivalent circuit of the electrical double layer shown in Fig. 3, which has been used previously to model the iron–acid surface.[3]

The electrolyte resistance R_s determined between reference and working electrodes can be obtained from the abscissa axis intercept of the semicircle at $f\rightarrow\infty$, $R_s = 1.5\,\Omega cm^2$, in all solutions studied. R_t is the charge-transfer resistance, and C_d is the double layer capacitance. The charge-transfer resistance R_t values are calculated from the difference in impedance at lower and higher frequencies, i.e., the diameter of the semicircle. In first approximation, C_d and the frequency f_{max} at which the imaginary component of the impedance is maximal ($-Z''_{max}$) are found as represented in Eq. (5):

$$f(-Z''_{max}) = \frac{1}{2\pi\tau_t}, \quad \text{where } \tau_t = R_t C_d \tag{5}$$

It may be assumed, as an approximation, that either $(R_t)^{-1}$ [19] or $(C_d)^{-1}$ [20] parameters are directly related to the corrosion rate. The inhibiting efficiency from the charge-transfer resistance is calculated as follows in Eq. (6):

$$E_{R_t}\% = \frac{R_{t/inh} - R_t}{R_{t/inh}} \times 100, \tag{6}$$

where R_t and $R_{t/inh}$ are the charge-transfer resistance values without and with inhibitor, respectively.

It can be expected that the R_t values increase with Q-CH_3 concentrations and that consequently the inhibition efficiency increases. This indicates that the charge-transfer process mainly controls the corrosion of mild steel. The values of double layer capacitance are brought down to the maximum extent in the presence of Q-CH_3, and the decrease of C_d follows the order similar to that obtained for i_{corr} in this study. This result is in favor of selective adsorption of Q-CH_3 in specific places[21] and/or formation of complex onto the metal surface.[22] According to this inhibition mechanism, Q-CH_3 could be adsorbed at active points, thus causing the corrosion rate to drop. The values of E_{R_t}% obtained from EIS measurements agree with those deducted from polarization and gravimetric methods.

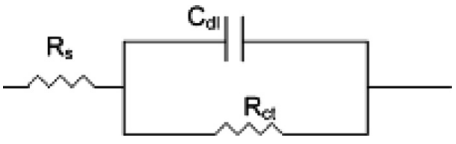

FIGURE 3 Equivalent circuit for the metal–acid interface.

Influence of Immersion Period

Fig. 4 presents the effect of immersion time on the impedance spectra at the corrosion potential. The inhibitor concentration was set at 10^{-2} M. The shape of these diagrams is very similar to that obtained when varying the inhibitor concentration. The effect of increasing immersion time on impedance spectra is characterized by the increasing size of the loop observed, reaching a maximum after 12 hr, and then it seems to be fairly constant afterward. The charge-transfer resistance (determined at the low frequency limit of the impedance spectrum) changes from about 329 Ωcm^2 after 0.5 hr to approximately 431 Ωcm^2 after 12 hr of immersion. At the same time, the capacitance values remain almost the same, approximately 20 $\mu F\,cm^{-2}$. These results demonstrate the formation of surface film and confirm those results obtained by the polarization curves.

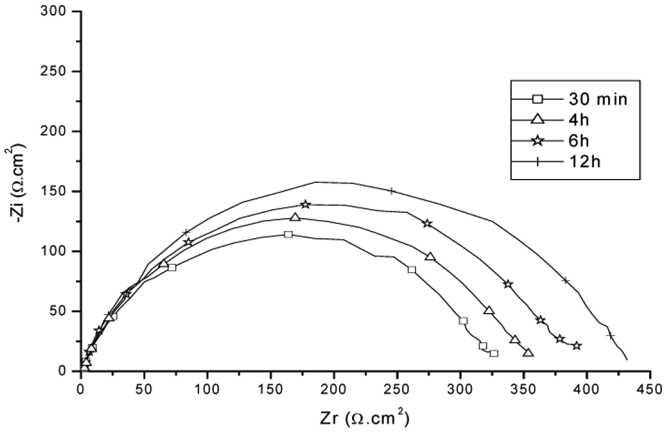

FIGURE 4 EIS spectra under open circuit conditions at different immersion time: System mild steel with 1M HCl + 10^{-2} M of Q-CH_3 at 293 K.

Effect of Temperature

We considered it worthwhile to study the effect of temperature as it can modify the interaction between the mild-steel electrode and the acidic medium in the presence and the absence of Q-CH_3. The interest in exploring the activation energy of the corrosion process and the thermodynamics of Q-CH_3 adsorption was developed by investigating the temperature dependence of the corrosion current densities using Tafel extrapolation method. Polarization curves for mild steel in 1M HCl without and with 10^{-2} mol L^{-1} of Q-CH_3 in the temperature range 293–323 K are shown in Fig. 5. The corresponding data are given in Table 4.

In the studied temperature range, the corrosion potential (E_{corr}) and the Tafel slope (β_c) are slightly modified in both uninhibited and inhibited media. The corrosion current density increases with the rise of temperature in both solutions and is markedly pronounced in the absence of Q-CH_3. The protection efficiency of this inhibitor decreases slightly with the rise of temperature. These results confirm that Q-CH_3 acts as an efficient inhibitor in the temperature range 293–323 K.

The corrosion reaction can be regarded as an Arrhenius process, the rate of which is given by Eq. (7):[23]

$$i_{corr} = A \exp\left(-\frac{E_a}{RT}\right), \qquad (7)$$

where A is the Arrhenius pre-exponential constant, E_a is the apparent activation energy of the corrosion process, R is the gas constant ($R = 8.314\,J K^{-1} mol^{-1}$), and T is the absolute temperature.

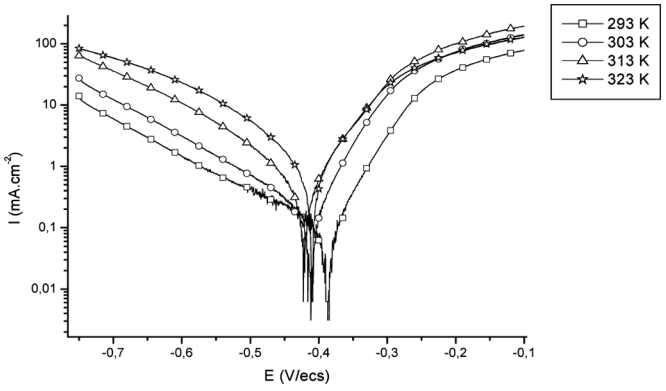

FIGURE 5 Effect of temperature on the cathodic and anodic responses for mild steel in 1M HCl added to 10^{-2} M of Q-CH_3.

TABLE 4 Electrochemical Characteristics of Mild Steel in 1M HCl With and Without 10^{-2} M of Q-CH_3 at Different Temperatures

Variable	Temperature (K)	E_{corr} (mV_{sce})	i_{corr} ($\mu A\ cm^{-2}$)	$\lvert\beta_c\rvert$ ($mV\ dec^{-1}$)	E_I (%)
Blank	293	−396	1072	125	–
	303	−395	2015	133	–
	313	−396	2158	140	–
	323	−404	2743	145	–
	333	−414	3420	181	–
Q-CH_3	293	−388	74	136	93
	303	−412	146	134	93
	313	−423	397	118	86
	323	−411	468	106	83

Kinetic parameters, such as enthalpy and entropy of corrosion process, may be evaluated from the effect of temperature. An alternative formulation of Arrhenius equation is called *transition state*[23] and is in Eq. (8):

$$i_{corr} = \frac{k_B T}{h} \exp\left(\frac{\Delta S^*}{R}\right) \exp\left(-\frac{\Delta H^*}{RT}\right), \qquad (8)$$

where k_B is the Boltzmann's constant ($k_B = 1.38066\ 10^{-23}\,J K^{-1}$), h is Planck's constant ($h = 6.6252\ 10^{-34}$ J s), and ΔH^* and ΔS^* are the enthalpy and the entropy of activation, respectively.

Figure 6 presents the Arrhenius plots of the logarithm of the current density versus 1/T, for mild steel in the corrosive medium with and without addition of 10^{-2} M of Q-CH_3. Straight lines are obtained with a slope of ($-E_a/R$). Figure 7 shows the plot of Ln (i_{corr}/T) against 1/T. Straight lines are obtained with a slope of ($-\Delta H^*/R$) and an intercept of ($\mathrm{Ln}\,k_B/h + \Delta S^*/R$), which give the values of ΔH^* and ΔS^*.

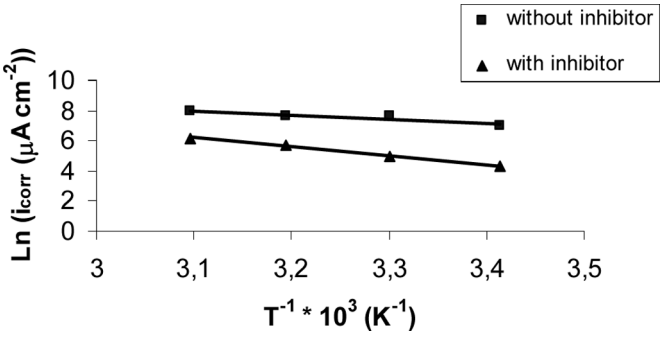

FIGURE 6 Arrhenius plots of mild steel in 1M HCl with and without 10^{-2} M of Q-CH_3.

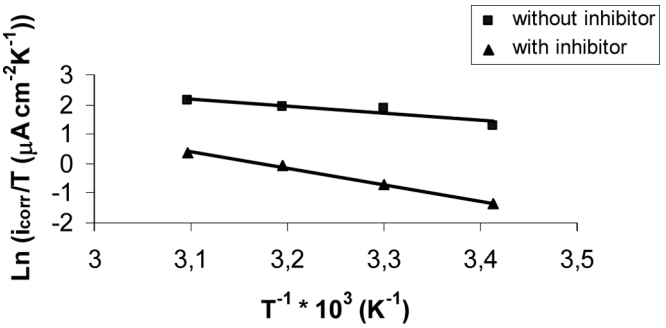

FIGURE 7 Arrhenius plots of Ln (i_{corr}/T) vs. 1/T in 1M HCl with and without 10^{-2} M of Q-CH_3.

Table 5 collects the values of activation parameters (E_a, ΔH^* and ΔS^*) for mild steel in the corrosive medium with and without addition of 10^{-2} of Q-CH_3.

Activation energy value obtained in the presence of Q-CH_3 is approximately double that obtained from the inhibitor free 1M HCl medium. Generally, the inhibitive additive causes rise in E_a value when compared to the blank, and this could often be interpreted as an indication for the formation of an adsorptive film by a physical (electrostatic) mechanism[25] or chemisorption.[26]

This high activation energy value supports the low value of i_{corr} deduced from the polarization measurements and indicates the higher protective efficiency of Q-CH_3. In the same way, the pre-exponential factor A like E_a increases in the presence of Q-CH_3 as reported by Reference.[27]

The positive values of ΔH^* mean that the dissolution reaction is an endothermic process and that the dissolution of steel is difficult.[28] Practically E_a and ΔH^* are the same order. This result enabled us to check the thermodynamic relation of Gomma and Wahdan[29] between E_a and ΔH^* as shown in Eq. (9):

$$E_a - \Delta H^* = RT. \tag{9}$$

The calculated value of the difference in the two solutions is 3 kJ mol^{-1}, which is close to the experimental value of RT, approximately 2.52 kJ mol^{-1} at 303 K. Also the entropy ΔS^* increases more negatively with the presence of Q-CH_3 than the noninhibited one. This reflects the formation of an ordered stable layer of Q-CH_3 onto the mild steel surface electrode.[30]

Adsorption Isotherm

The adsorption isotherm provides useful insights into the mechanism of corrosion inhibition. The surface coverage, θ, given in Table 2, was calculated according to Eq. (10).

$$\theta = \frac{i_{corr} - i_{corr/inh}}{i_{corr}} = \frac{E_I\%}{100} \tag{10}$$

Surface coverage values for the Q-CH_3 were obtained from the current–voltage measurements at 10^{-2} M of Q-CH_3 at 293 K. Several adsorption isotherms were assessed. The best fitted straight line (Fig. 8) is obtained from the plot of C_{inh}/θ versus C_{inh} with slope of 1.008 around unity. The regression coefficient is $r^2 = 0.9984$. This suggests that the Q-CH_3 adsorption on the metal surface obeyed the Langmuir's adsorption isotherm.[31]

$$\frac{C_{inh}}{\theta} = \frac{1}{K_{ads}} + C_{inh}, \text{ with } K_{ads} = \frac{1}{55,55}\exp\left(-\frac{\Delta G^\circ_{ads}}{RT}\right), \tag{11}$$

where K_{ads} is the adsorption coefficient or adsorption equilibrium constant, and ΔG°_{ads} is the standard free energy of adsorption. The calculated equilibrium constant of Q-CH_3 adsorption reaction is 43421.66 mol$^{-1}\cdot$L, which lead to $\Delta G^\circ_{ads} = -35.79$ kJ mol^{-1}. The negative value of ΔG°_{ads} indicates the spontaneous adsorption of Q-CH_3 on the steel surface.[32] More, the negative value of ΔG°_{ads} suggests the strong interaction of Q-CH_3 molecule on the metal surface.[33]

Values of ΔG°_{ads} up to -20 kJ mol^{-1} are consistent with the electrostatic interaction between the charged molecules and the charged metal (physisorption).

TABLE 5 Values of Activation Parameters E_a, ΔH^* and ΔS^* for Mild Steel in 1M HCl and Addition of 5×10^{-3} M of Q-CH_3

Concentration (mol L^{-1})	Pre-exponential factor, A (μA cm^{-2})	E_a (kJ mol^{-1})	ΔH^* (kJ mol^{-1})	ΔS^* (JK^{-1} mol^{-1})
Blank	14.7×10^6	22.9	22.8	−49.5
5×10^{-3}	4.4×10^{10}	49.2	52.2	−116.3

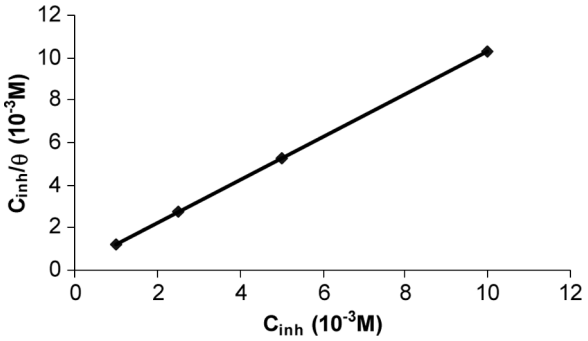

FIGURE 8 **Langmuir adsorption isotherm plot for mild steel in 1M HCl at different concentrations of Q-CH_3.**

CONCLUSION

Concluding the experimental part, it was clearly demonstrated that all techniques used, especially electrochemical techniques, are able to characterize and follow the inhibition of the corrosion process promoted by 6-methylquinoxalin-2(1H)-one (Q-CH_3) molecules. It was shown that this compound is a good inhibitor for mild steel in 1M HCl solution with efficiencies of around 97% at a concentration of 10^{-2} M. The electrochemical impedance diagrams showed mainly a capacitive loop, which can be attributed to the formation of an adsorbed layer on the steel surface. The thermodynamic parameters indicated that the inhibitor is physisorbed on the metal surface and that its adsorption obeys the Langmuir adsorption isotherm.[34,35]

REFERENCES

1. Mernari, B.; Elkadi, L.; Kertit, S. *Bulletin of Electrochemistry* **2001**, *17*, 115.
2. Bentiss, F.; Bouanis, M.; Mernari, B.; Traisnel, M.; Vezin, H.; Lagreneé, M. *Applied Surface Science* **2007**, *253*, 3696.
3. Popova, A.; Christov, M.; Zwetanova. A. *Corrosion Science* **2007**, *49*, 2131.
4. Lagrenée, M.; Mernari, B.; Chaibi, N.; Traisnel, M.; Vezin, H.; Bentiss, F. *Corrosion Science* **2001**, *48*, 951.
5. Schmitt, G. *Corrosion and Corrosion Control* **1984**, *19*, 165.
6. Benmessaoud, Es-salah, M. K.; Hajjaji, N.; Takenouti, H.; Srhiri, A.; Ebn Touhami, M. *Corrosion Science* **2007**, *49*, 3880.
7. Hosseini, M.; Mertens, S. F. L.; Ghorbani, M.; Arshadi, M. R. *Materials Chemistry and Physics* **2003**, *78*, 800.
8. Young-Seuk, H.; Hyun-Muk, K.; Yong-Tae, P.; Ho-Sik, K. *Bulletin Korean Chemistry Society* **2000**, *21*, 133.
9. El Mehdi, B.; Mernari, B.; Traisnel, M.; Bentiss, F.; Lagrenée, M. *Materials Chemistry and Physics* **2002**, *77*, 489.
10. Li, W.; He, Q.; Pei, C.; Hou, B. *Electrochim. Acta* **2007**, *52*, 6386.
11. Popova, A.; Christov, M.; Vasilev, A. *Corrosion Science* **2007**, *49*, 3290.
12. Dehri, Ï.; Özcan, M. *Materials Chemistry and Physics* **2006**, *98*, 316.
13. Rosenfeld, I. L. *Corrosion Inhibitors*; McGraw-Hill: New York, 1981.
14. Cole, K.S.; Cole, R.H. *Journal of Chemistry and Physics* **1941**, *9*, 341.
15. Duval, S.; Keddam, M.; Sfaira, M.; Srhiri, A.; Takenouti, H. *Journal of Electrochemical Society* **2002**, *149*, B520.
16. Davidson, D. W.; Cole, R. H. *Journal of Chemistry and Physics* **1951**, *19*, 1484.
17. Juttner, K. *Electrochim. Acta* **1990**, *35*, 1501.
18. Deflorain, F.; Miscovic-Stankovic, V. B.; Bonora, P. L.; Fedrizzi, L. *Corrosion* **1994**, *50*, 446.
19. Gao, G.; Liang, C. H.; Wang, H. *Corrosion Science* **2007**, *49*, 1833.
20. Lagrenée, M.; Mernari, B.; Bouanis, M.; Traisnel, M.; Bentiss, F. *Corrosion Science* **2004**, *44*, 573.
21. Bastidas, J. M.; Polo, J. L.; Cano, E.; Torres, C. L. *Journal of Material Science* **2000**, *35*, 2637.
22. Abboud, Y.; Abourriche, A.; Saffaj, T.; Berrada, M.; Charrouf, M.; Bennamara, A.; Al Himidi, N.; Hannache, H. *Materials Chemistry and Physics* **2007**, *105*, 1.
23. Putilova, I. N.; Balezin, S. A.; Barannik, V. P. *Metallic Corrosion Inhibitors*; Pergamon Press: Oxford, 1960.
24. Bockris, J. O'M.; Reddy, A. K. N. *Modern Electrochemistry*; Plenum Press: New York, 1977; vol. 2, 1267.
25. Popova, A.; Sokolova, E.; Raicheva, S.; Christov, M. *Corrosion Science* **2003**, *45*, 33.
26. Szauer, T.; Brandt, A. *Electrochim. Acta* **1981**, *22*, 1209.
27. Mu, G. N.; Li, X. M.; Li, F. *Materials Chemistry and Physics* **2004**, *86*, 59.
28. Guan, N. M.; Xueming, L.; Fei, L. *Materials Chemistry and Physics* **2004**, *86*, 59.
29. Gomma, G. K.; Wahdan, M. H. *Materials Chemistry and Physics* **1995**, *39*, 209.
30. Yurt, A.; Balaban, A.; Kandemir, S. U.; Bereket, G.; Erk, B. *Materials Chemistry and Physics* **2004**, *85*, 420.
31. Langmuir, I. *Journal of the American Chemical Society* **1947**, *39*, 1848.
32. Talati, J. D.; Gandhi, D. K. *Corrosion Science* **1983**, *23*, 1315.
33. Tang, L.; Li, X.; Li, L.; Qu, Q.; Mu, G.; Liu, G. *Materials Chemistry and Physics* **2005**, *94*, 353.
34. Benabdellah, M.; Touzani, R.; Aouniti, A.; Dafali, A.; El Kadiri, S.; Hammouti, B.; Benkaddour, M. *Materials Chemistry and Physics* **2007**, *105*, 373.
35. Quraishi, M. A.; Rawat, J.; Ajmal, M. *Journal of Applied Electrochemistry* **2000**, *30*, 745.